

## SWAP Calibration Information

This document describes the calibration incorporated into the data pipeline (level 3), and information included in the SWAP calibration directory, which is necessary for further data processing (level 4 and higher). Currently, the pipeline includes calibration information to perform the background subtraction for all plan 0 and plan 3 measurements, and to calculate then energy labels for the spectrograms. The energy bins were calculated using an instrument model, which combined all the calibration information discussed in this document. Since the energy bins were calculated assuming ions entered the instrument in the center of the instrument, and the energy does not depend on some quantities such as the geometric factor, the energy bin calculations are primarily a function of the RPA and ESA response curves. The additional information discussed required for further data processing include: the instrument field of view, angular responses of the RPA and ESA, deflector calibration, and geometric factor. Much of the calibration data is discussed in the SWAP instrument paper. We refer to some figures in the instrument paper, and provide some further details necessary to work with our data.

### *1) Retarding Potential Analyzer (RPA)*

The RPA response curve is shown in Figure 29 of the SWAP instrument paper over the full voltage range of the instrument. To obtain a smooth average shape several tests were used. Since each test had a different beam flux, the count rates for each test were normalized by the number of count rate at the RPA cut-off. The RPA cut-off is where the slope is the steepest. Likewise some of the tests had slightly different beam energies; therefore the x-axis is the RPA voltage normalized by the beam energy. The RPA grids consists of holes drilled in metal, and act as a series of electrostatic lenses. This causes dips and peaks not typical of wire mesh grids. Such features occur at RPA voltage to beam energy ratios less than 0.95. In the calibration directory we include the RPA response curve file (rpa\_shape.tab).

The RPA response also depends on the azimuth ( $\alpha$ ) angle that the ions enter the instrument. Figure 1 defines the azimuth angle to be positive towards the top of the

instrument and negative toward the bottom of the instrument. Ideally, non-normal incident particles with  $E/q > (V_{RPA} / \cos^2\alpha)$  would be passed; however, the focusing properties of the SWAP RPA lead to a more complex response function. In Figure 30 of the instrument paper the normalized response of the RPA as a function of the azimuth angle is shown. Below is a formula for the RPA voltage scaled by the incident beam energy ( $f$ ) as a function of the azimuth angle.

$$\begin{aligned}
 f &= \cos^2(2\alpha), & \alpha &\leq 4.0 \\
 f &= \cos^2(3.5\alpha - 10) - 0.03, & 4.0 < \alpha &\leq 10 \\
 f &= \cos^2(5.5\alpha - 65) - 0.085, & 10 < \alpha &
 \end{aligned}$$

For SWAP non-normal incident particles with  $E/q > (V_{RPA} / f(\alpha))$  are transmitted through the RPA.

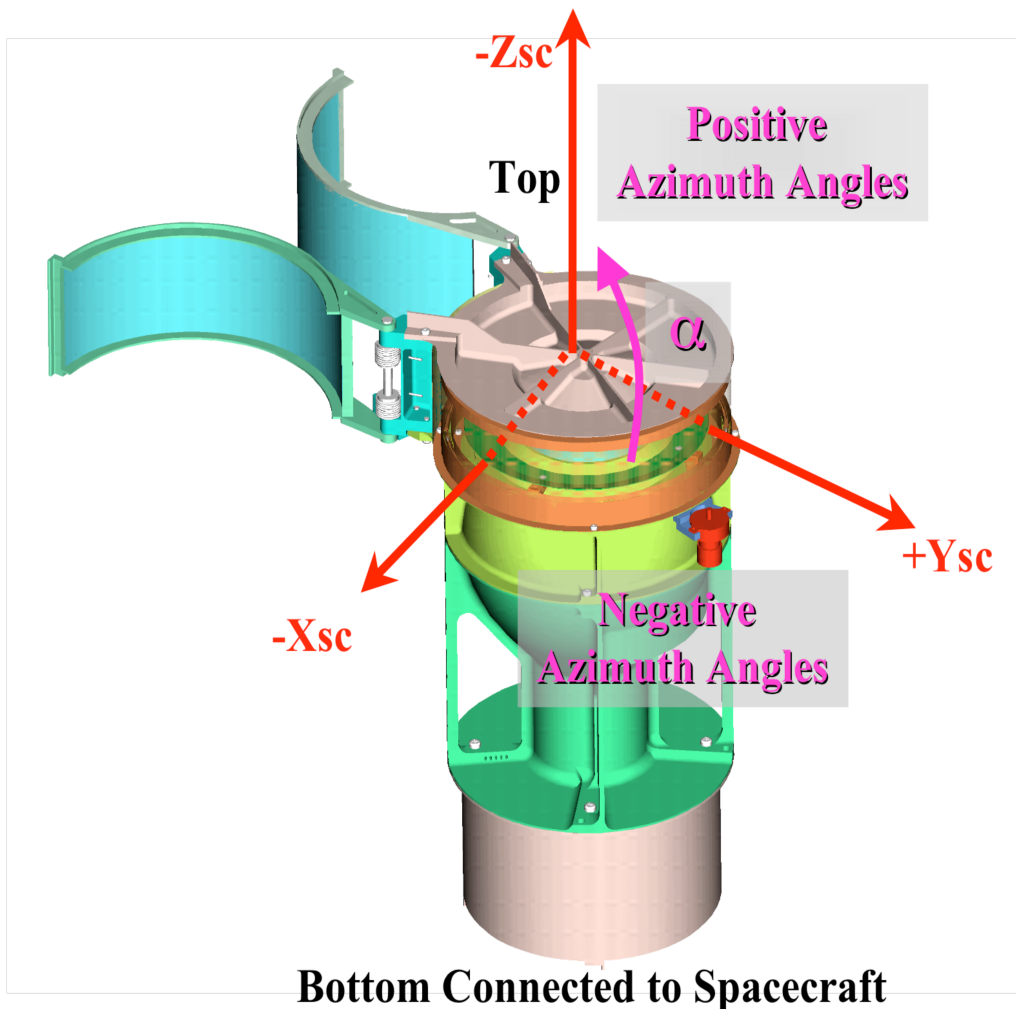


**Figure 1:** Diagram defining the azimuth angle. Bottom of the instrument connects to the spacecraft.

## 2) Deflector System (DFL)

We have used the deflector only a small amount of time during commissioning, in particular during the angle test. The deflector is an electrostatic deflection plate between the RPA and the ESA. It is used to adjust the Field Of View (FOV). It can increase the FOV out of plane away from the spacecraft by up to  $15^\circ$  in azimuth ( $\alpha$ ). The deflector was calibrated in the lab by changing the deflector voltage and turning the instrument so that the ions enter at different angles. The resulting formula for the deflector voltage normalized by the beam energy is a polynomial in azimuth angle.

$$\frac{V_{\text{deflector}}}{E_{\text{beam}}} = 0.007 \alpha^2 + 0.0209 \alpha + 0.1009 \quad (1)$$

## 3) Electrostatic Analyzer (ESA)

Both the center and width of the electrostatic analyzer (ESA) response curve vary with the azimuth angle. Figure 31 in the instrument paper shows an example of the energy-azimuth angle response of the ESA to a 1keV proton beam. The factor to convert the ESA voltage to energy, the analyzer constant, is 1.88 at an azimuth and roll angle of zero. The energy resolution  $\Delta E/E$  is 8.5%, and the angular FOV, undeflected, is  $10^\circ$  in the azimuth direction. We include the ESA response curve in the calibration directory (`esa_shape.tab`). In Figure 2 below we show the response curve where the y-axis is the count rate normalized by the peak count rate and the x-axis is the ESA voltage normalized by the center of the response.

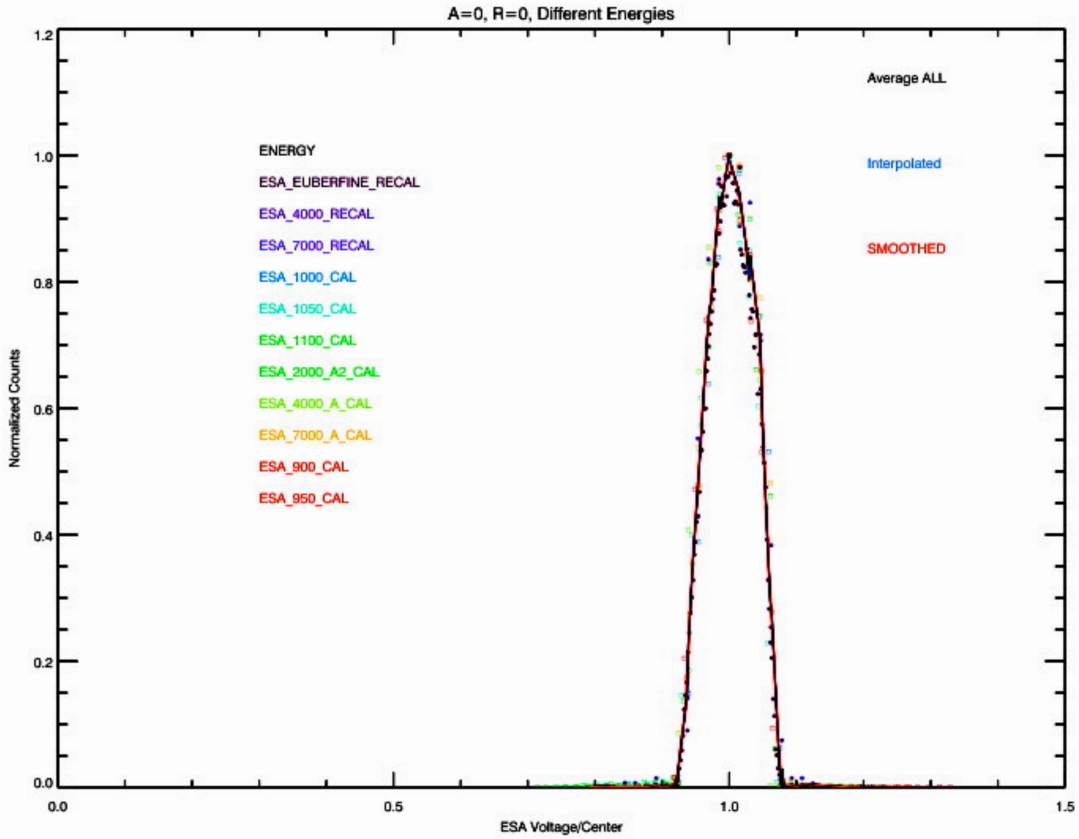


**Figure 2:** ESA Response function: Normalized counts versus ESA voltage normalized by the ESA voltage at the peak response.

The ESA width varies with azimuth angle. We fit many ESA response curves taken at different energies and azimuth angles, and found the full width at half max (FWHM) as a function of azimuth angle. We then normalized the widths by the ESA voltage (center of the ESA response) and averaged over many tests taken at different energies. Below we show these averages plotted as a function of azimuth angle (Figure 3), and we show the results in tabular form in Table 1.

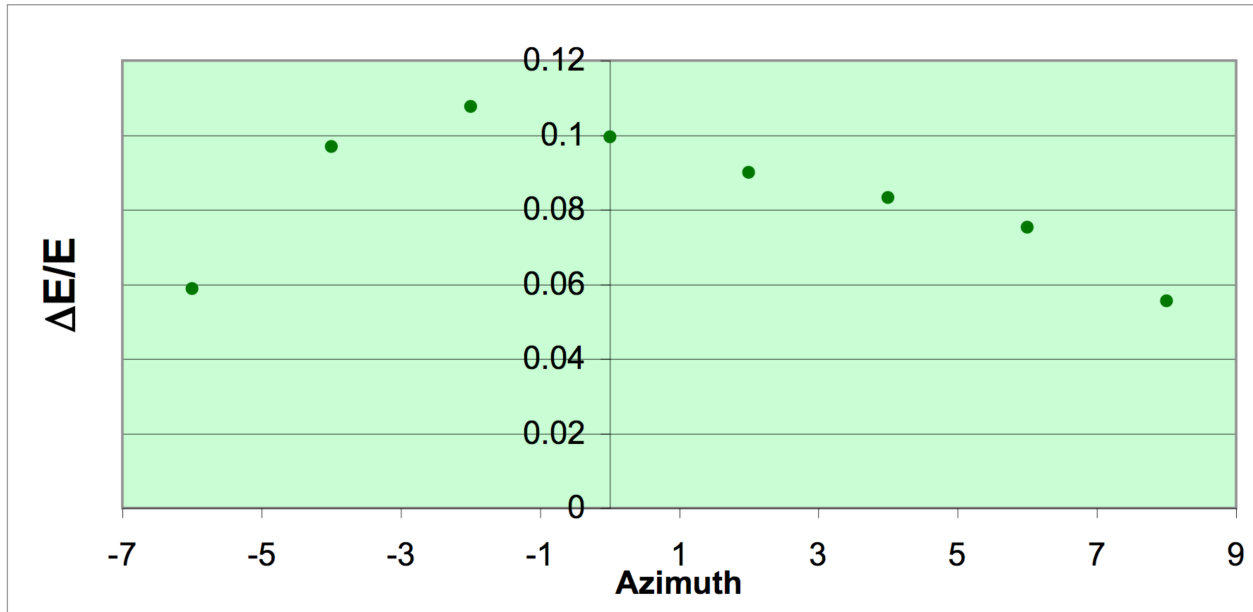


**Figure 3:** Ratio of the ESA response width (FWHM) normalized by the center of the ESA response as a function of azimuth angle [deg].

**Table 1:** Normalized ESA width (FWHM) versus azimuth angle

$\Delta E/E$	Azimuth [deg]
0.0588	-6
0.0970	-4
0.1077	-2
0.0995	0
0.0900	2
0.0833	4
0.0754	6
0.0556	8

We determine the k-factor (inverse of the analyzer constant), which is the ratio between the ESA voltage and the beam energy, by examining the ratio of the ESA voltage to the beam energy at different azimuth and roll angles (Figure 4). Looking down on the top of the instrument the roll ( $\varphi$ ) angle is in the X-Y spacecraft plane with positive roll angles towards the +Xsc axis and the negative roll angles towards the -Xsc axis (Figure 5). The k-factor was found to be a linear function of the azimuth angle ( $k=b+m\alpha$  where b are the intercepts and m are the slopes), but different linear responses are observed at different

roll angles. Below is a table of slopes and intercepts a different roll angles.

Roll Angle [deg]	$m(\alpha < 0)$ [deg <sup>-1</sup> ]	$b(\alpha < 0)$	$m(\alpha > 0)$ [deg <sup>-1</sup> ]	$b(\alpha > 0)$
-90	-0.0010849	0.538471	-0.00477399	0.537755
0	0.00036525	0.530168	-0.00489876	0.527318
90	-0.000227406	0.529935	-0.00491875	0.528725

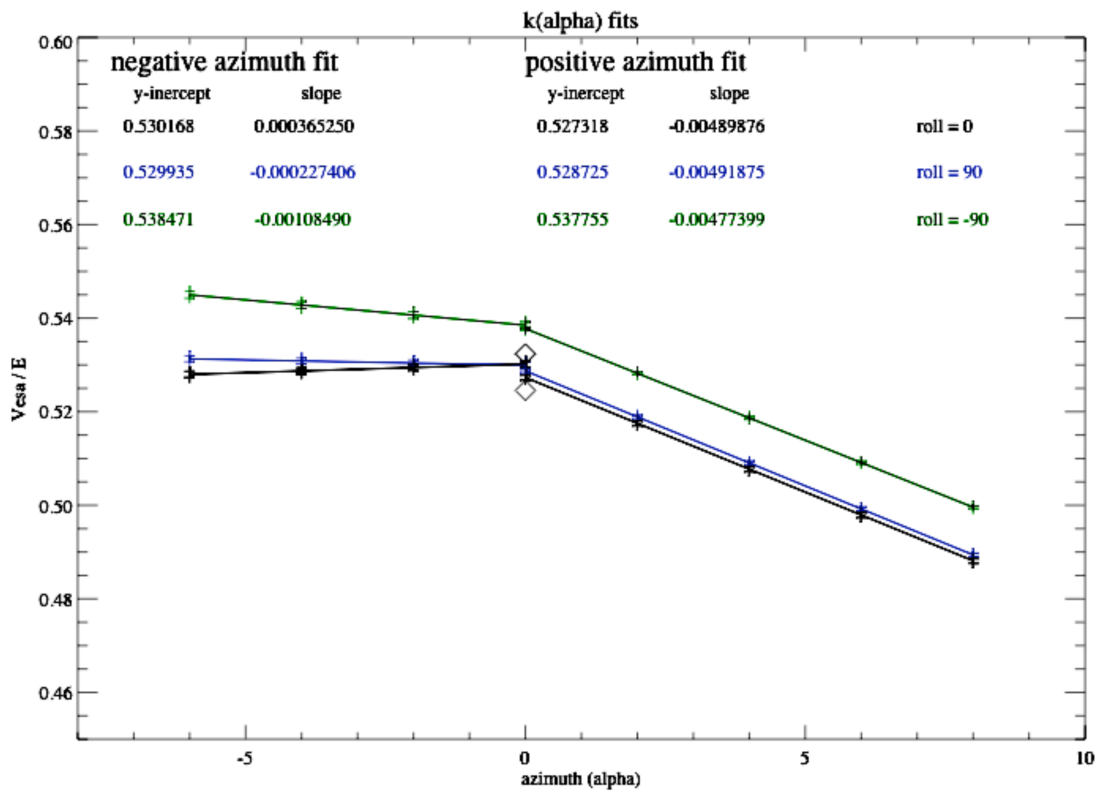


**Figure 4:** The ratio of the ESA voltage to the beam energy at different azimuth angles [deg] on the x-axis and roll angles shown as different curves.

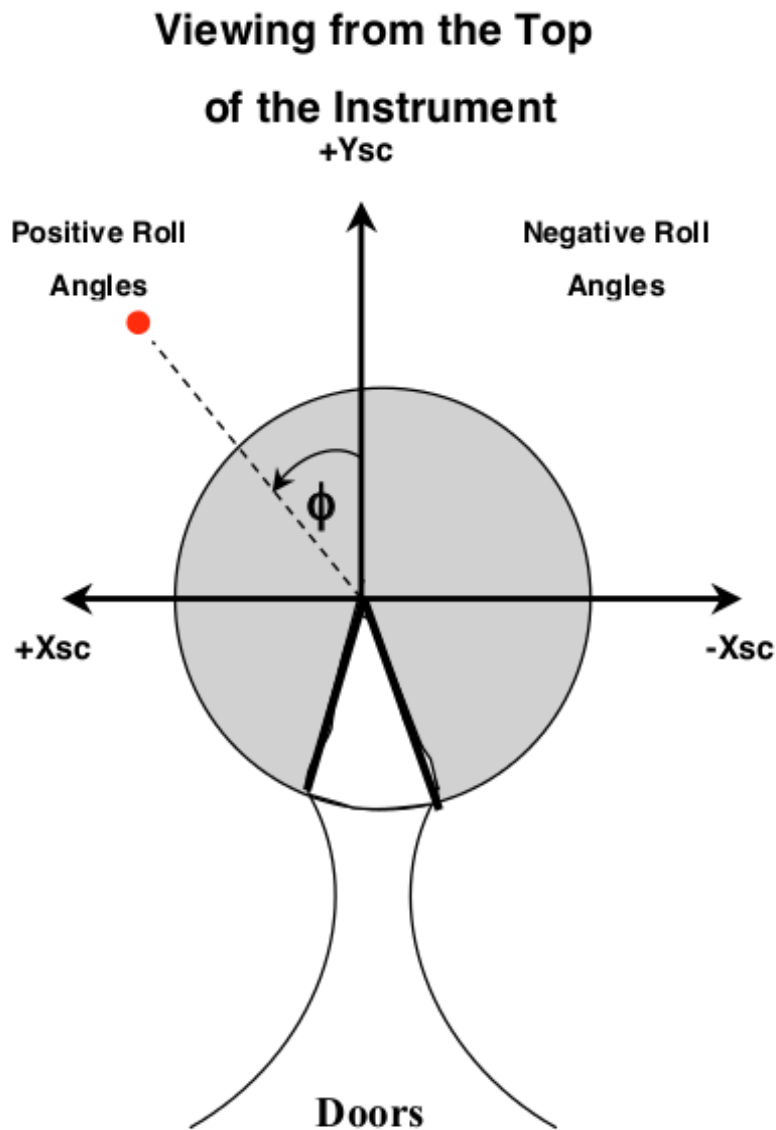


**Figure 5:** Diagram defining the roll ( $\phi$ ) angle. The view is looking at the top of the instrument towards the spacecraft.

#### 4) Energy Bin Calculations

The location of the energy bin peak response is calculated using the instrument model, which is based on many different functions and parameters determined in the calibration. The energy bin peak response depends on the voltage settings of the RPA, ESA, DFL and the angle the ion enter. For science observations in the Jupiter phase, the deflector voltage was zero except during the angle test. Since we do not know what angle the ions enter, we assume the ions enter the center of the instrument; this assumption limits the uncertainty in the location of the center of the ESA passband to about 10% for ions

entering anywhere in the 10° instrument Field-Of-View (see Figure 31 of [MCCOMASETAL2008]). We then use the RPA and ESA voltage setting to calculate the center of the combined response. We have the energy of the peak response for each RPA and ESA voltage setting in the onboard voltage tables. In the calibration directory we list the filenames of the precalculated energy bin centers and the time periods over which they are valid in the `list_energy_files.tab` file. Each energy bin file (i.e., `esa_rpa_v19_energy_binsf.csv`, filename suffix extension is `.tab` in PDS data sets) lists the plan number, sweep, number, ESA DAC, RPA DAC, ESA voltage, RPA voltage, the crossing ratio (ratio of the RPA voltage to the ESA center energy), energy at the peak response, energy width (FWHM), minimum energy, and maximum energy. These energy tables are used to determine the energy in the spectrograms.

### 5) Detectors

The gain on the detectors can be adjusted by adjusting the operating voltage of the detectors. The operation voltage was determined in the lab by sweeping the voltage while illuminating the instrument with a constant intensity 1 keV proton source. Figure 32 of the instrument paper shows the lab calibration results were the response of the PCEM, SCEM, and the COIN rates are given as a function of voltage. The operation voltage was selected to be 2100 V at start of mission since at that voltage the CEM gain curves are on saturated. The instrument gain naturally degrades with age and usage, and we will perform regular gain tests to determine if the voltage needs to be adjusted. The gain also affects the geometric factor and effective area. In the table below we list the effective areas and geometric factors for the PCEM, SCEM, coincidence and a combined detection in the PCEM,SCEM, or coincidence.

<b>Detection Signal</b>	<b>Geometric Factor</b>	<b>Effective Area</b>
PCEM	4.1e-3 cm <sup>2</sup> sr eV/eV	0.058 cm <sup>2</sup>
SCEM	8.6e-3 cm <sup>2</sup> sr eV/eV	0.12 cm <sup>2</sup>
Coincidence	1.8e-3 cm <sup>2</sup> sr eV/eV	0.025 cm <sup>2</sup>
Any detection	1.1e-2 cm <sup>2</sup> sr eV/eV	0.15 cm <sup>2</sup>



## 6) Field of View (FOV)

In order to determine the field of view of the ESA, the RPA is turned off and the beam was fixed at one energy, and then the beam was moved to different roll and azimuth angles. The counts were recorded at each roll and azimuth setting until the full field of view of the instrument was covered. The field of view map is 1 degree resolution in azimuth angle and 4 degrees in roll angle. The map is a 2-D array of counts in roll and azimuth. Below we show this array normalized by the count rate in the bin at 0 degrees azimuth and -6 degrees roll (Figure 6). We provide a field of view map (fov\_mask\_2d.tab) for higher level data processing in the calibration directory.

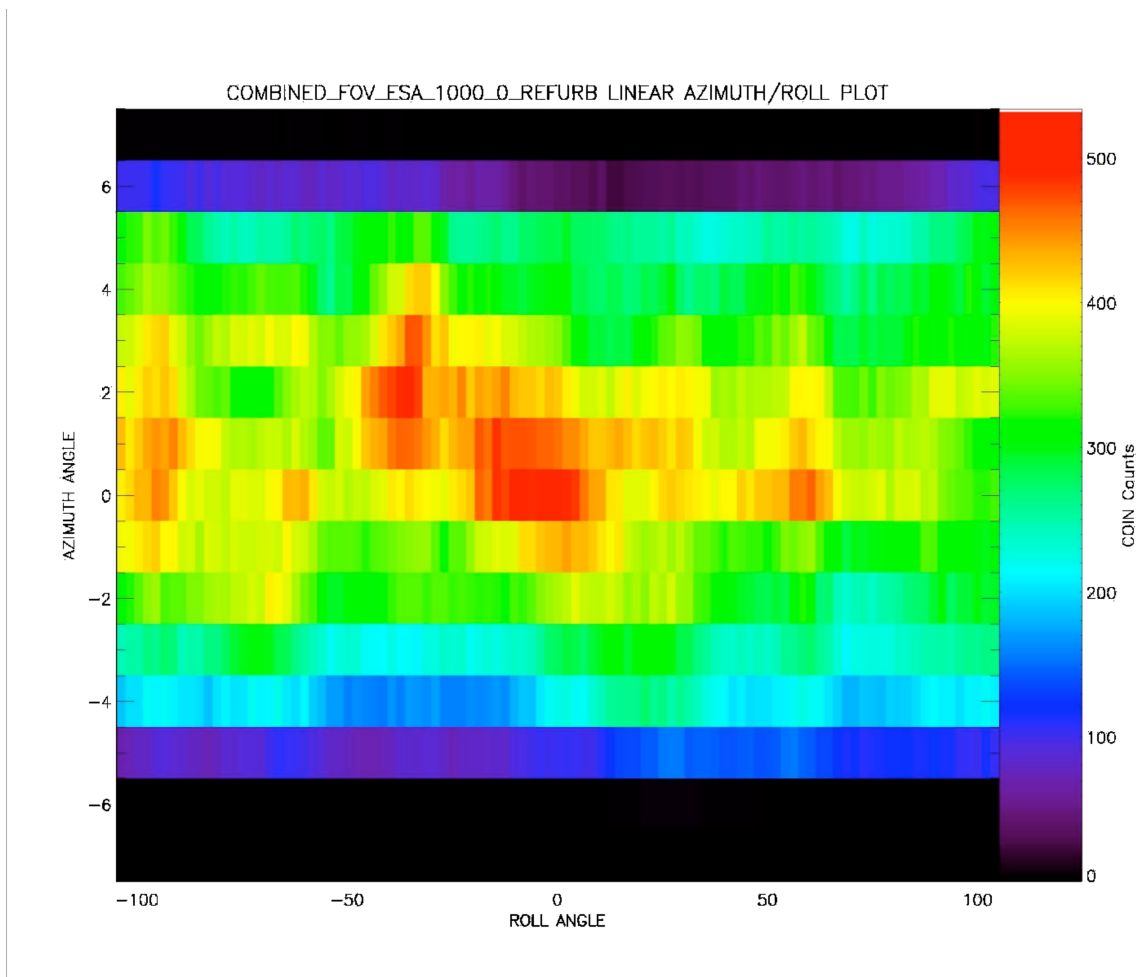


**Figure 6:** Field of View of the ESA: Normalized counts in color as a function of roll angle [deg] (x-axis) and azimuth [deg] (y-axis).

## 7) Background Subtraction

When the RPA is operating there is a background that needs to be removed. During the Jupiter phase we use plan 0/sweep 0 and plan 5/sweep 5 where the plans and sweeps refer to the RPA and ESA voltage tables. In plan 5 we do not use the RPA; consequently, there is no background to remove. In plan 0 we do need to remove the background. The background varies with the distance to the Sun. The current background files are based

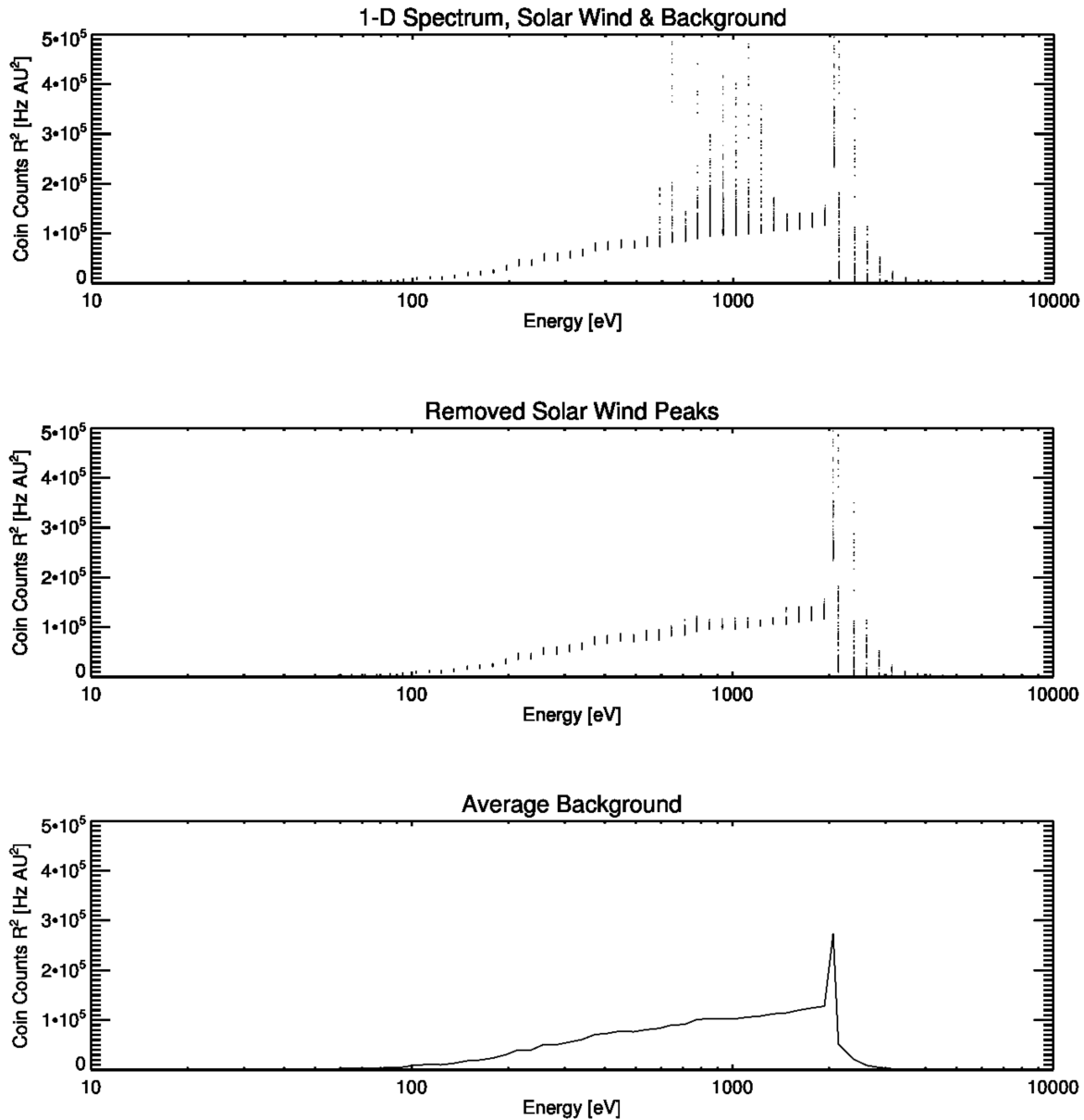


**Figure 7:** In the top panel the SWAP-009-6 coincidence count rates in Hz times the distances from the Sun, in AU, squared are shown as a function of energy. The middle panel is the same data with the spikes removed. The data is then binned and averaged (bottom panel).

on calibration measurements taken during the sequence SWAP-009-6. In Figure 7 we show the SWAP-009-6 data for days 290-292, 299-301, 304-309, 316-318, 320-321, 335-339, 343- 344 used to create the background files. Here we plot the count rates in Hz times the square of the distance from the Sun in AU ( $R_{\text{Sun,AU}}$ ) versus the energy. Most of the vertical spikes are the solar wind peaks. In the middle panel the solar wind peak and 3 points below and above the energy of the peak have been removed from each scan individually. The bottom panel of Figure 7 is an average of the top bin where the average has been performed on each bin individually since there are a different number of data points in each bin after removing the solar wind peaks.

To use the background information in the pipeline the data was converted from Hz back to counts/sample since the background subtraction is done prior to the rest of the data processing. The background rates (counts / sample) are scaled by the square of the distance to the Sun ( $R_{\text{Sun,AU}}$ ) and those scaled rates (counts \*  $(R_{\text{Sun,AU}})^2$  / sample) are stored in the background files in the calibration directory. To remove the background we first scale the measured count rates by the distance to the Sun squared, and then subtract scaled background rates. After the subtraction the result is then divided by the distance to the Sun squared to obtain the rates in units of counts per sample. The background filenames and the time range for each file are listed in the list\_background\_files.tab file. The background file used during the Jupiter phase is called background\_009\_dac\_jup.tab. The background files contain the peak energy, ESA DAC, RPA DAC, PCEM background, SCEM background, and coincidence background rates in counts \*  $(R_{\text{Sun,AU}})^2$  / sample .